

# ROBUST $H_\infty$ CONTROL OF QUARTER-CAR SEMI-ACTIVE SUSPENSIONS

Olivier SENAME<sup>◇</sup> \*, Luc DUGARD<sup>+</sup>

<sup>◇</sup> INRIA Rhône-Alpes, 655 avenue de l'Europe, Montbonnot, 38 334 Saint-Ismier Cedex, FRANCE

Fax: +33 4.76.61.54.77, e-mail:Olivier.Sename@inrialpes.fr

<sup>+</sup> Laboratoire d'Automatique de Grenoble, ENSIEG-BP 46, 38402 Saint Martin d'Hères Cedex, FRANCE

Fax: +33 4.76.82.63.88, e-mail:Luc.Dugard@inpg.fr

**Keywords:** Automotive control, semi-active suspension,  $H_\infty$  control,  $\mu$ -analysis.

## Abstract

This paper deals with single-wheel suspension car model. The benefits of controlled semi-active suspensions compared to passive ones are here emphasized. The contribution relies on robust analysis of a  $H_\infty$  controller which improves comfort and road holding of the car under industrial specifications. Simulations on an exact nonlinear model of the suspension are performed for control validation.

## 1 Introduction

This paper is devoted to quarter car suspension models, which are a good representation for studying comfort and tyre rebound. Many control approaches such as optimal control, skyhook control, etc, have been applied to this type of model [3, 4, 1, 6]. An  $H_\infty$  control approach is proposed here for controlled semi-active suspensions which consist of a spring and an electronically controlled damper, in parallel. However, the damper can only dissipate energy, as is mostly the case in the automotive industry. The control issue is then to modify accurately the damping coefficient in real-time.

The  $H_\infty$  controller is designed following industrial oriented control objectives, i.e. industrial performance specifications and control validation on a nonlinear simulation model of the semi-active suspension. A robust stability and performance analysis of the designed controller is performed using the  $\mu$ -tool.

The paper is organized as follows. In section 2, the quarter-car model, i.e. the bounce model, is presented. A control-oriented linear model is described as well as the considered nonlinear simulation model of semi-active suspensions. The performance specifications are then described. Section 3 is devoted to  $H_\infty$  control design. A frequency analysis is proposed to point out, on the control model, the improvements due to the resulting controller. Section 4 presents a  $\mu$ -analysis of Robust Stability and Performance of the  $H_\infty$  controller. Finally section 5 presents the simulation results in the realistic framework of the nonlinear simulation model. The proposed control methodology is compared with a passive suspension (referred

to as the open loop case) upon the industrial performance objectives. The last section describes our conclusion.

## 2 The suspension model

The quarter-car model includes the chassis and the axle (see figure 1). It includes the vertical motions of the chassis (sprung mass  $m_s$ ) and of the axle (unsprung mass  $m_u$ ). The suspension is located between the axle and the chassis and consists of a damper (represented here by the force  $u$ ) and a spring ( $k_s$ ). The tyre is represented by a spring  $k_u$  only; indeed, the damping coefficient of a tyre is small and may be omitted for control purposes. The disturbance input is  $z_r$  the road profile.  $z_s$ ,  $z_u$  and  $z_r$  represent the positions of the sprung mass, of the unsprung mass and of the road excitation respectively, around the steady state operations.

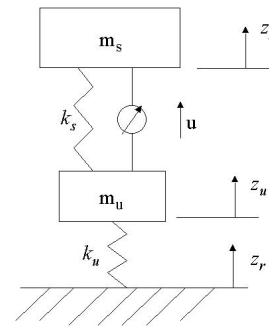


Figure 1: The quarter-car suspension.

### 2.1 Modelling

From fig 1, it leads:

$$m_s \ddot{z}_s = k_s(z_u - z_s) + u \quad (1)$$

$$m_u \ddot{z}_u = k_s(z_s - z_u) - u + k_u(z_r - z_u) \quad (2)$$

with  $m_s = 415kg$ ,  $m_u = 52kg$ ,  $k_s = 22000N/m$  and  $k_u = 270000N/m$ . For the control design,  $u$  is considered in (1-2) as:

$$u = c(\dot{z}_u - \dot{z}_s) + v \quad (3)$$

where  $c$  is constant and positive and  $v$  represents the contribution of the (controlled) active force added to the passive one. Thus, a passive suspension corresponds to  $v = 0$  (i.e. the open

\*This work was done when the first author was at the Laboratoire d'Automatique de Grenoble, France. Olivier.Sename@inpg.fr

loop case), and an active one when  $v$  is the output of a controller (closed-loop case). In this case, the damper is an active actuator. However it does not take into account the force limitation due to the suspension deflection speed ( $\dot{z}_u - \dot{z}_s$ ). The control validation will be performed on the following nonlinear model of a semi-active suspension.

$$\begin{cases} m_s \ddot{z}_s &= f_{k_s}(z_u - z_s) + f_u \\ m_u \ddot{z}_u &= f_{k_s}(z_s - z_u) - f_u + f_{k_u}(z_r - z_u) \end{cases} \quad (4)$$

where  $f_{k_s}$  and  $f_{k_u}$  are nonlinear functions described by static maps, and  $f_u$  is as follows:

- passive suspension :  $f_u$  is positive but depends on the suspension deflection speed. In this industrial oriented application, it is then defined by a static map identified from experimental data  $f_u = f_c(\dot{z}_u - \dot{z}_s)$ , represented in figure 2(a).
- semi-active suspension:  $f_u$  can change but is limited by upper and lower values that depend on the suspension deflection speed. Here, the number of possible values for the friction coefficient is finite. They are represented on figure 2(b) by static maps identified from experimental data. In the control step, the applied force  $f_u = f_{sa}(v, \dot{z}_u - \dot{z}_s)$  is chosen to be as closed as possible to  $v$  the force required by the controller for a given suspension deflection speed.

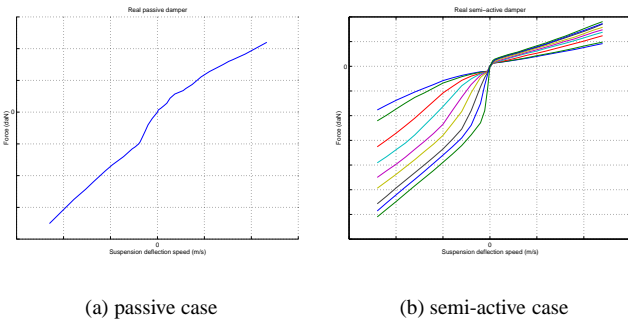


Figure 2: Force-Speed Characteristics

Then, in the case of semi-active suspensions, the limitations of the force  $f_u$  that the damper can generate entail some unavoidable deteriorations of the results obtained in the purely active case of the control-oriented model. Let us note that these limitations are not only due to the saturations on the deliverable force of the damper, but also and mainly, to the physical characteristics of the damper, the generated force of which belongs to a fixed range depending on the suspension deflection speed.

## 2.2 Industrial performance specifications

The analysis of vehicle ride (particularly the comfort) involves the study of the ride excitation sources, the human response to vibration, and the vibrational behaviour of the vehicle [2, 9]. We are mainly interested here in improving the comfort of the

vehicle without deterioration of the road holding. For quarter-car models, the road holding can only be studied by the vertical behaviour of the tyre (i.e. the wheel bounce), which only represents a small part of the road handling (that should take into account the longitudinal and lateral motions). As far as vibration isolation is concerned, the comfort can be evaluated from the vertical response of the chassis, which is a fair index of passenger comfort. Considering chassis acceleration should be closed to human response to vibration, but is neither completely representative of comfort which, relative to human response, also includes the perception and tolerance of vibrations. In the following we present two main criteria that represent the required industrial control objectives.

**Vibration isolation.** It is evaluated by the displacement of the sprung mass with respect to the excitation from the ground input.

For this test, the road profile is a  $\pm 15mm$  sine, with varying frequency in  $[0 - 5]Hz$ .

In the ideal case, the vertical displacement of the chassis should be the same as the one of the road for low frequencies (lower than around  $1Hz$ ) and should be null for high frequencies (higher than around  $1Hz$ ). In practice, the maximal gain of the transfer function from the road displacement to the chassis displacement (occurring between 1 and  $5Hz$ ) has to be limited to 2. Moreover, for a good damping of the oscillations in the human body sensitivity frequency range, the filtering ability of this transfer function has to be kept (for frequencies higher than the frequency of the peak, i.e. around  $1 - 2Hz$ ) even if the maximal gain is reduced.

**Road holding.** As indicated before, it is evaluated from the unsprung mass displacement with respect to the road surface.

For this test, the road profile is a sine of magnitude  $\pm 1mm$  in the frequency range  $[0 - 20]Hz$ .

For a good road holding, the maximal gain (in the range  $8 - 15Hz$ ) of the considered transfer function has to be limited to 2.

## 3 $H_\infty$ control approach

### 3.1 Some background on $H_\infty$ control

This part states the problem in a way similar to [8] where more details can be found.

$H_\infty$  control is formulated using the general control configuration (I) in figure 3 where  $\mathcal{P}(s)$  is the generalized plant model,  $w$  is the exogenous input vector,  $v$  is the control input vector,  $e$  is the controlled output vector,  $y$  is the measurement vector.

Given  $\gamma$ , a prespecified attenuation level, an  $H_\infty$  suboptimal control problem is to design a controller that internally stabilizes the closed-loop system and ensures:

$$\|N_{ew}(s)\|_\infty \leq \gamma \quad (5)$$

where  $N_{ew}(s)$  is the closed-loop transfer matrix from  $w$  to  $e$ . The minimal value  $\gamma_{opt}$  is then approached by a bisection algo-

rithm.

In general, some weights are considered on the controlled outputs (including the actuator force). They represent the performance specifications in the frequency-domain.  $\mathcal{P}$  thus includes the plant model  $G$  and the considered input and output weights ( $W_i, W_o$ ) as in figure 3 (II).

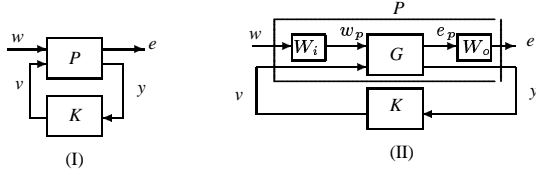


Figure 3: General control configuration

The  $H_\infty$  control problem is then referred to as a mixed sensitivity problem,  $W_i$  and  $W_o$  thus appearing in (5) as weights on the sensitivity functions. The usual way of solving the  $H_\infty$  control problem is the use of Riccati equations or LMI. This leads to the design of the control law  $v$  that solves the suboptimal problem (5). A bisection algorithm is then used to approach the minimal value of  $\gamma$ .

### 3.2 The $H_\infty$ suspension control design

More details on this part are given in [7]. The considered control model is given in (3), where  $c$  is chosen as some medium linear value of the passive suspension on fig 2(a):  $c = 1500Ns/m$ . The measured output is the suspension deflection ( $z_s - z_u$ ) only, which is widely used in automotive industry because of its low cost and simplicity. The feedback structure is presented in figure 4.

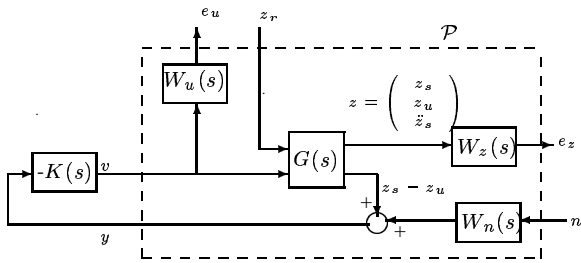


Figure 4: The control scheme including the weighting functions

It includes the weighting functions, the suspension control model  $G(s)$  and the controller  $K(s)$  to be designed. According to Figures 3 and 4,  $v$  is the control input to be designed,  $y = z_s - z_u + n$  is the measured output and  $w = [z_r \quad n]^T$  represents the external disturbance inputs. The global controlled outputs are  $e = (e_z^T, e_u^T)^T$ , where  $e_u = W_u v$  is the weighted control input and  $e_z = W_z z$  the weighted controlled output with  $z = [z_s \quad z_u \quad \ddot{z}_s]^T$  (the output weight on figure 3 (II) is then  $W_o = \text{diag}(W_u, W_z)$ ). The measurement noise  $n$  has been normalized using the input weight  $W_i = W_n$ . As the controlled outputs are  $z = [z_s, z_u, \ddot{z}_s]^T$ , the matrix  $W_z$

of weighting functions is chosen as:

$$W_z = \text{diag}(W_{z_s}, W_{z_u}, W_{z_s2nd})$$

The weighting functions ( $W_z, W_u, W_n$ ) have been chosen according to the industrial performance specifications. They are described below in more details, and presented on figure 5.

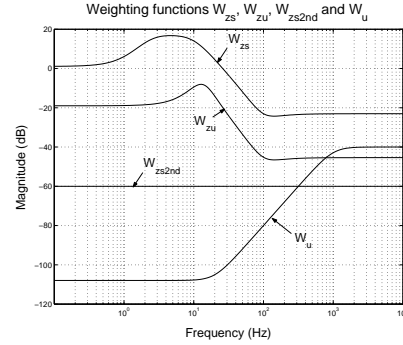


Figure 5: Weighting functions  $W_{z_s}$ ,  $W_{z_u}$  and  $W_{z_s2nd}$  applied on the displacements of the chassis, of the axle and on the chassis acceleration

**$W_{z_s}$ :** The inverse of the weighting function  $W_{z_s}$  defines the template of the transfer function  $z_s/z_r$ . In particular the resonance peak at around 1Hz of the open loop system is limited. As it corresponds to a second order transfer function with a damping coefficient lower than  $\sqrt{2}$ , the weighting function is chosen so that the associated template is a second order with a greater damping coefficient (0.9) at this frequency (1Hz).

Due to the structure of the model, the transfer function  $z_s/z_r$  has an invariant point at 11Hz. Moreover the system has a natural filtering effect after 10Hz. Thus  $z_s$  is not constrained beyond 10Hz to keep some freedom degrees for the remaining control objectives.

**$W_{z_u}$ :** In the case of the transfer function  $z_u/z_r$ , only the decrease of the resonance peak around 10Hz is needed for the road holding specification. The frequency range of interest is relatively narrow, so second order filters are used with small damping coefficients (0.4 and 0.6) in order to obtain narrow resonance peak of the weighting function  $W_{z_u}$ .

**$W_u$ :** the control input  $v$  is weighted beyond (20Hz) according to the actuator limitations in high frequencies.

**$W_{z_s2nd}$  and  $W_n$ :** In order not to increase the controller complexity, the weighting functions acting on the chassis acceleration and on the measurement noise are chosen constant ( $w_{z_s2nd}$  and  $w_n$  respectively).

Using the chosen weighting functions, the  $H_\infty$  control problem has a solution. The transfer functions of the closed loop and open loop systems, as well as the associated templates, are given in figures 6 to 9. Figures 6 to 8 allow to compare the

open loop system, the closed loop system and the templates for the three transfer functions  $z_s/z_r$ ,  $z_u/z_r$  and  $\ddot{z}_s/z_r$ . The transfer function  $v/z_r$  of the closed loop system and the associated template are represented on figure 9. These figures show that the  $H_\infty$  controller improves the suspension performances compared with the passive one (i.e. the open-loop case).

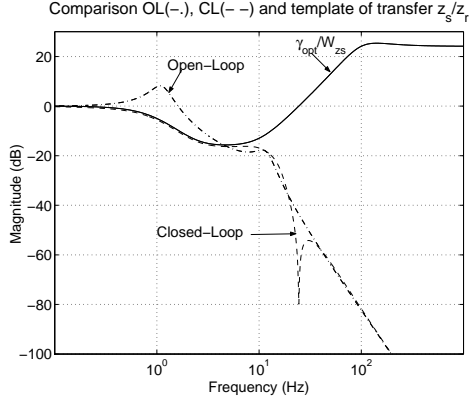


Figure 6:  $z_s/z_r$

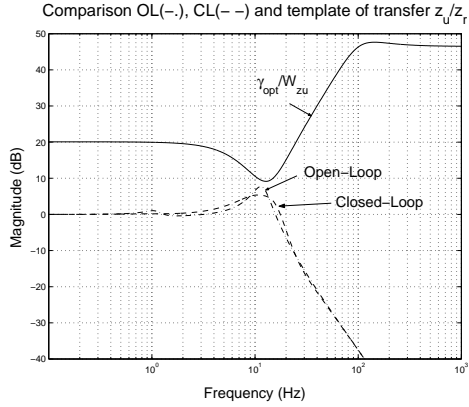


Figure 7:  $z_u/z_r$

## 4 Robust stability and performance analysis

Many details about the methodology used in this part may be found in Zhou [10], Skogestad and Postlethwaite [8].

Roughly speaking, a control system is robust if it is insensitive to differences between the actual real system and the model used to design the controller. Let us recall that, in addition to nominal stability and performance, the objectives of any control system include:

**Robust Stability (RS).** The system is stable for all perturbed plants about the nominal model up to the worst-case model uncertainty.

**Robust Performance (RP).** The system satisfies the performance specifications for all perturbed plants about the nominal model up to the worst-case model uncertainty.

In the current application, the class of uncertainties we are in-

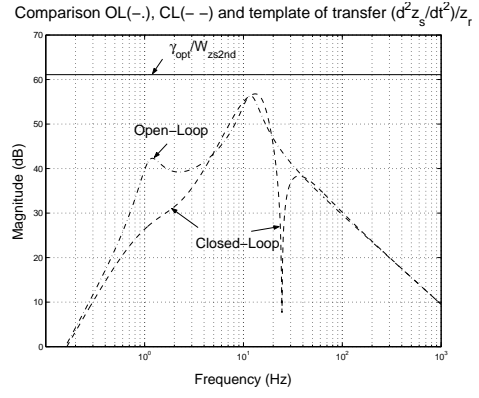


Figure 8:  $\ddot{z}_s/z_r$

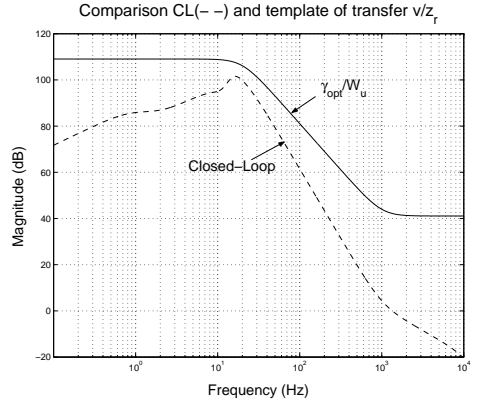


Figure 9:  $v/z_r$

terested in, is parametric uncertainties. In particular, the masses and spring stiffness are considered to be badly known. In the considered suspension model (1-2), the sprung mass is the most varying parameter, depending mainly on the number of passengers, car load ... The other parameters will vary due to industrial manufacturing only. The uncertainties are therefore represented as:

$$\begin{aligned} \overline{m_s} &= m_s(1 + p_{m_s}\delta_{m_s}), & p_{m_s} &= 30\%, & \delta_{m_s} &\in [-1; 1] \\ \overline{k_s} &= k_s(1 + p_{k_s}\delta_{k_s}), & p_{k_s} &= 10\%, & \delta_{k_s} &\in [-1; 1] \\ \overline{k_u} &= k_u(1 + p_{k_u}\delta_{k_u}), & p_{k_u} &= 10\%, & \delta_{k_u} &\in [-1; 1] \\ \overline{m_u} &= m_u(1 + p_{m_u}\delta_{m_u}), & p_{m_u} &= 10\%, & \delta_{m_u} &\in [-1; 1] \end{aligned}$$

Using ad hoc LFT representations of the parametric uncertainties, we can pull out the perturbations in a  $4 \times 4$  diagonal block as [10]:  $\Delta_r = \text{diag}\{\delta_{k_s}, \delta_{k_u}, \delta_{m_s}, \delta_{m_u}\}$ .

### 4.1 Background on RS and RP analysis

The starting point of the robustness analysis is the block-diagonal representation of the uncertainties set:

$$\underline{\Delta} = \{\text{diag}\{\Delta_1, \dots, \Delta_q, \delta_1 I_{r_1}, \dots, \delta_r I_{r_r}, \epsilon_1 I_{c_1}, \dots, \epsilon_c I_{c_c}\} \in \mathbb{C}^{k \times k}, \Delta_i \in \mathbb{C}^{k_i \times k_i}, \delta_i \in \mathbb{R}, \epsilon_i \in \mathbb{C}\}.$$

where  $\Delta_i(s)$ ,  $i = 1, \dots, q$ , represent full block complex uncertainties,  $\delta_i(s)$ ,  $i = 1, \dots, r$ , real parametric uncertainties, and  $\epsilon_i(s)$ ,  $i = 1, \dots, c$ , complex parametric uncertainties.

Taking into account the uncertainties leads to the following General Control Configuration on figure 10,

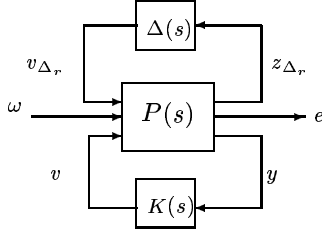


Figure 10: General control configuration with uncertainties

where  $\Delta \in \underline{\Delta}$ . Here, only real parametric uncertainties (given in  $\Delta_r$ ) are considered for RS analysis. RP analysis also needs a fictive full block complex uncertainty, as in figure 11, where

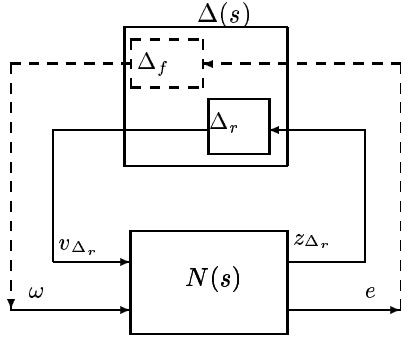


Figure 11:  $N\Delta$

$N(s) = \begin{bmatrix} N_{11}(s) & N_{12}(s) \\ N_{21}(s) & N_{22}(s) \end{bmatrix}$ , and the closed-loop transfer matrix is:

$$T_{ew}(s) = N_{22}(s) + N_{21}(s)\Delta(s)(I - N_{11}(s))^{-1}N_{12}(s) \quad (6)$$

Note that in (6),  $N_{22}(s) = N_{ew}$  is the nominal closed-loop transfer matrix. If it is stable, the instability in (6) may only come from  $(I - N_{11}(s))^{-1}$ .

As we consider structured uncertainties, a  $\mu$ -analysis is used to study RS and RP. First the structured singular value is defined as:

$$\mu_{\underline{\Delta}}(M)^{-1} := \min\{\bar{\sigma}(\Delta) : \Delta \in \underline{\Delta}, \det(I - \Delta M) \neq 0\}.$$

For RS, we shall determine how large  $\Delta$  (in the sense of  $H_{\infty}$ ) can be without destabilizing the feedback system. From (6), the feedback system becomes unstable if  $\det(I - N_{11}(s)) = 0$  for some  $s \in \mathbb{C}, \Re(s) \geq 0$ . The result is then the following.

**Theorem 1** [8] *Assume that the nominal system  $N_{ew}$  and the perturbations  $\Delta$  are stable. Then the feedback system is stable for all allowed perturbations  $\Delta$  such that  $\|\Delta(s)\|_{\infty} < 1/\beta$  if and only if  $\forall \omega \in \mathbb{R}, \mu_{\underline{\Delta}}(N_{11}(j\omega)) \leq \beta$ .*

Assuming nominal stability, RS and RP analysis for structured uncertainties are therefore such that:

$$\text{RS} \Leftrightarrow \mu_{\Delta_r}(N_{11}) < 1, \forall \omega \quad (7)$$

$$\text{RP} \Leftrightarrow \mu_{\Delta}(N) < 1, \forall \omega, \Delta = \begin{bmatrix} \Delta_f & 0 \\ 0 & \Delta_r \end{bmatrix} \quad (8)$$

Finally, let us remark that the structured singular value cannot be explicitly determined, so that the method consists in calculating an upper bound and a lower bound, as closed as possible to  $\mu$ .

## 4.2 RS and RP for $H_{\infty}$ suspension control

An upper bound of  $\mu$  for RS and RP is given on figures 12 and 13. As  $\mu(M) \leq 0.31$ , RS is satisfied. Hence the  $H_{\infty}$  controller

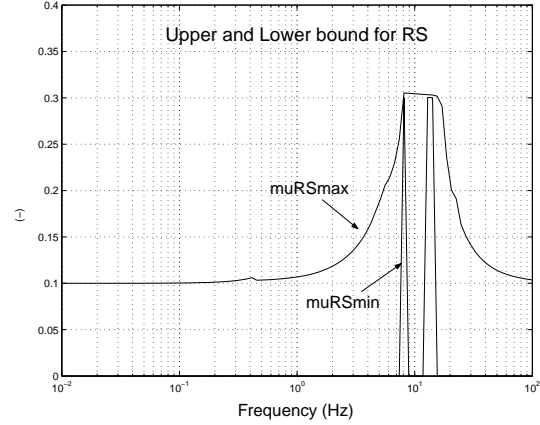


Figure 12: Upper and Lower bound for RS

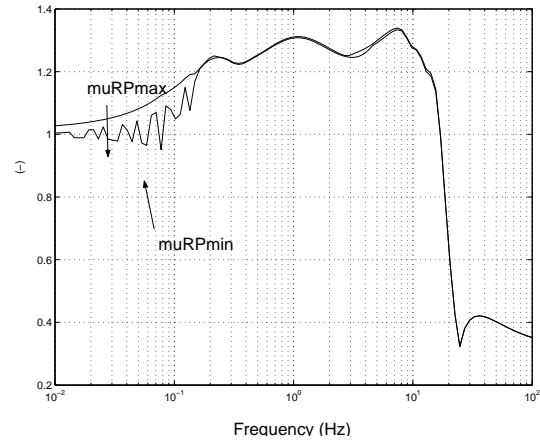


Figure 13: Upper and Lower bound for RP

keeps stability for the considered uncertainties. Moreover, this means that the closed-loop system remains stable for larger uncertainties, i.e.:

$$m_s = 415kg \pm (30/0.31)\% = 415kg \pm 97\%$$

$$m_u = 52kg \pm (10/0.31)\% = 52kg \pm 32\%,$$

$$k_s = 22000N/m \pm 32\%, \quad k_u = 270000N/m \pm 32\%.$$

On the other hand as  $\mu(N) < 1.34$ , we cannot conclude on Robust Performance in this uncertainty case. However one could check that RP is satisfied for lower uncertainties as:

$$m_s = 415kg \pm 22, \quad m_u = 52kg \pm 7.5\%$$

$$k_s = 22000N/m \pm 7.5\%, \quad k_u = 270000N/m \pm 7.5\%.$$

Note also that, even if the uncertainties on  $m_s$  may be very

large, it can be, in practice, estimated when the car is stopped (before riding) so that a damper force can be added to compensate the car load. The steady state of the car can then be recovered.

## 5 Control validation

Simulations are here provided using the nonlinear model to emphasize the benefits of  $H_\infty$  controlled semi-active suspensions, in a more realistic framework.

**Vibration isolation:** Compared to the passive suspension, the semi-active suspension improves both the resonance peak and the filtering ability. The comfort is improved using the  $H_\infty$  controller.

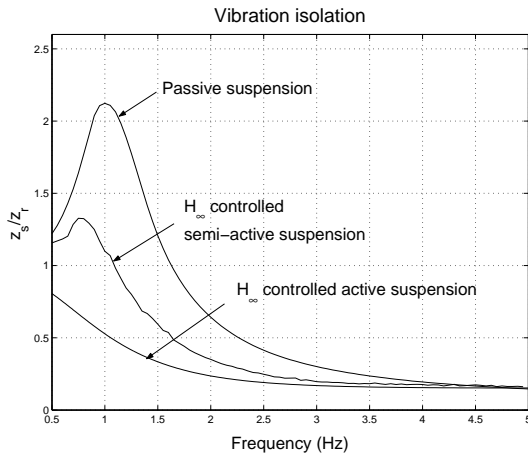


Figure 14: frequency-response from road input ( $z_r$ ) to vertical displacement of chassis ( $z_s$ )

**Road holding:** The  $H_\infty$  controlled semi-active suspension approximately provides the same road holding as the passive suspension.

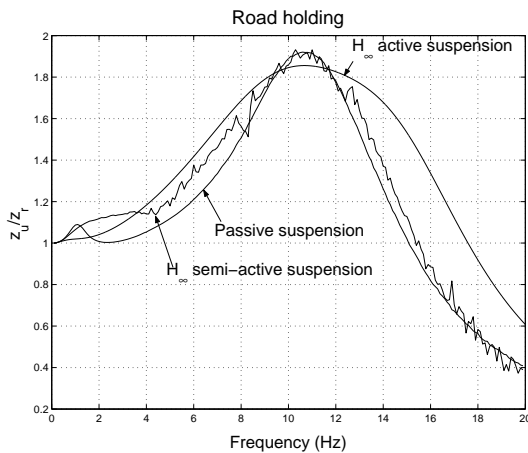


Figure 15: frequency-response from road input ( $z_r$ ) to vertical displacement of axle ( $z_u$ )

Therefore  $H_\infty$  approach seems to be a good choice for control of semi-active suspensions.

## 6 Concluding remarks

This paper has dealt with  $H_\infty$  control design, for a quarter-car model, under industrial performance specifications.

A Robust Stability and Performance analysis has been provided. This points out that the  $H_\infty$  controller remains stable for large uncertainty (in particular 100% for the sprung mass). Concerning Robust Performance, the performance specifications are kept for parameter uncertainties up to 22% for the sprung mass and 7.5% for the remaining masses and stiffness. This is quite good as the sprung mass can be measured in practice when the car is stopped.

By applying the  $H_\infty$  controllers on a exact nonlinear simulation model, the improvement in comfort is emphasized. Road holding is, according to the industrial performance specifications, almost equivalent to the passive suspension case.

The results thus show the interest of  $H_\infty$  control for semi-active car suspensions.

**Acknowledgements** Some parts of this work were sponsored by PSA Peugeot-Citroën, and are drawn from Sammier's PhD Thesis [5].

## References

- [1] M.M. Elmadany and Z.S. Abduljabbar. Linear quadratic gaussian control of a quarter-car suspension. *Vehicle System Dynamics*, 32:479–497, 1999.
- [2] T. D. Gillespie. *Fundamentals of vehicle dynamics*. Society of Automotive Engineers, Warrendale, USA, 1992.
- [3] D. Hrovat. Applications of optimal control to advanced automotive suspension design. *ASME Journal of Dynamic Systems, Measurement and Control*, pages 328–342, 1993.
- [4] A. Liberzon, P.O. Gutman, and D. Rubenstein. Active control for single-wheel suspension of off-road track vehicle. *IFAC Workshop on Motion Control*, pages 105–110, September, 21–23 1998. Grenoble, France.
- [5] D. Sammier. *On modelling and control of automotive car suspension (in french)*. PhD thesis, INPG - LAG, 2001. [www-lag.ensieg.inpg.fr](http://www-lag.ensieg.inpg.fr).
- [6] D. Sammier, O. Sename, and L. Dugard. Comparison of skyhook and  $h_\infty$  control applied on a quarter-car suspension model. *IFAC Workshop on Advances in Automotive Control*, March 2001. Karlsruhe, Germany.
- [7] D. Sammier, O. Sename, and L. Dugard. Skyhook and  $h_\infty$  control of semi-active suspensions: some practical aspects. *Vehicle System Dynamics*, 39(4):279–308, April 2003.
- [8] S. Skogestad and I. Postlethwaite. *Multivariable Feedback Control*. John Wiley and Sons, 1996.
- [9] J.Y. Wong. *Theory of Ground Vehicles*. John Wiley and Sons, New York, second edition edition, 1993.
- [10] K. Zhou. *Essentials of robust control*. Prentice Hall, New Jersey, 1998.